Journal of the European Ceramic Society **19** (1999) 1255–1258

PII: S0955-2219(98)00415-4
0955-2219/99/$ - see front matter

Pyroelectric $PbZrO_3$-based Ceramics Prepared Through Hot Isostatic Pressing

O. Sugiyama,[a]* S. Saito,[a] K. Kato,[b] S. Osumi,[b] K. Murakami[c] and S. Kaneko[c]

[a]Shizuoka Industrial Research Institute, Makigaya, Shizuoka 421-1221, Japan
[b]Fuji Ceramics Co., Yamamiya, Fujinomiya 418-0111, Japan
[c]Ceramics Research Group, Shizuoka University, Johoku, Hamamatsu 432-8561, Japan

Abstract

A novel pyroelectric ceramic was successfully prepared by means of a hot isostatic pressing (HIP) technique using a mixture of two perovskite $PbZrO_3$-based powders. The temperature dependence of the enhanced pyroelectric coefficient, $9{\cdot}4\times10^{-4}\,Cm^{-2}\,°C^{-1}$, of this ceramic was almost flat over a temperature range between 15°C and 70°C, while the two starting materials and their solid solution were temperature dependent. Surface layers of several hundreds nm thick were formed on the grains and have a compositional gradient corresponding to mutual substitution of B-site ions between the starting materials. It was found that the control of the temperature dependence of the pyroelectricity resulted from overall integration of each characteristic pyroelectric coefficient in the compositional gradient region. Finally, the structural model of the HIP sample could tentatively be proposed.

Keywords: hot isostatic pressing, microstructure-final, PZT, sensors.

1 Introduction

Ferroelectric lead zirconate based ceramics are promising materials as pyroelectric detectors.[1,2] It is known that a strong increase in the pyroelectric sensitivity can be observed around the phase transition temperature between the two ferroelectric phases of rhombohedral $Pb(Zr,Ti)O_3$ (PZT) ceramics, labeled as $F_{LT}(R)$ and $F_{HT}(R)$.[3–6] A control of this abrupt increase holding high sensitivity is desirable for practical applications. Some attempts for the reduction of the temperature dependence have been made through the formation of a multilayered structure or the liquid-phase sintering, however, the pyroelectric peak did not disappear completely.[7–9]

The authors discovered the disappearance of this peak, without the deterioration of the level of the pyroelectric sensitivity for $PbZrO_3$-based ceramics, which were prepared using hot isostatic pressing (HIP) technique.[10] The microstructural characteristic of this sample would be responsible for this effect. In this study, the relationship between the pyroelectricity and the microstructure of the hot isostatic pressed $PbZrO_3$-based ceramics have been investigated and compared to the cases of starting materials and conventionally sintered materials.

2 Experimental

Preparation procedure of samples in this study is shown in Fig. 1. The nominal compositions of starting materials for HIP were $Pb(Mn_{1/3}Nb_{2/3})_{0.1}Zr_{0.9}O_3 + 0{\cdot}5\,wt\%\ MnO_2 + 0{\cdot}5\,wt\%\ Cr_2O_3$ (abbreviated hereafter as P1) and $Pb(Mn_{1/3}Nb_{2/3})_{0.1}Zr_{0.875}Ti_{0.025}O_3 + 0{\cdot}5\,wt\%\ MnO_2 + 0{\cdot}5\,wt\%\ Cr_2O_3$ (P2), showing respective phase transition temperatures around 30°C and 50°C. First $Pb(Mn_{1/3}Nb_{2/3})_{0.1}Zr_{0.9}O_3$ and $Pb(Mn_{1/3}Nb_{2/3})_{0.1}Zr_{0.875}Ti_{0.025}O_3$ powders were obtained by calcining the mixtures of corresponding oxides at 900°C for 2 h, then by mixing with MnO_2 and Cr_2O_3 for the preparation of P1 and P2. The shaped samples were sintered at 1280°C for 3·5 h after the pre-sintering at 850°C for 2 h. Two kinds of samples were prepared through the hot isostatic pressing (900°C, 98 MPa, 2 h; abbreviated hereafter as HIP) and the conventional sintering (1280°C, 3·5 h; CS), respectively, of the equimolar mixture of P1 and P2. The hot isostatic pressing was performed in Ar atmosphere with the glass encapsulation method using a Petri dish.[10]

*To whom correspondence should be addressed. Fax: 81 53 428 4160; e-mail: osamu@h-iri.pref.shizuoka.jp

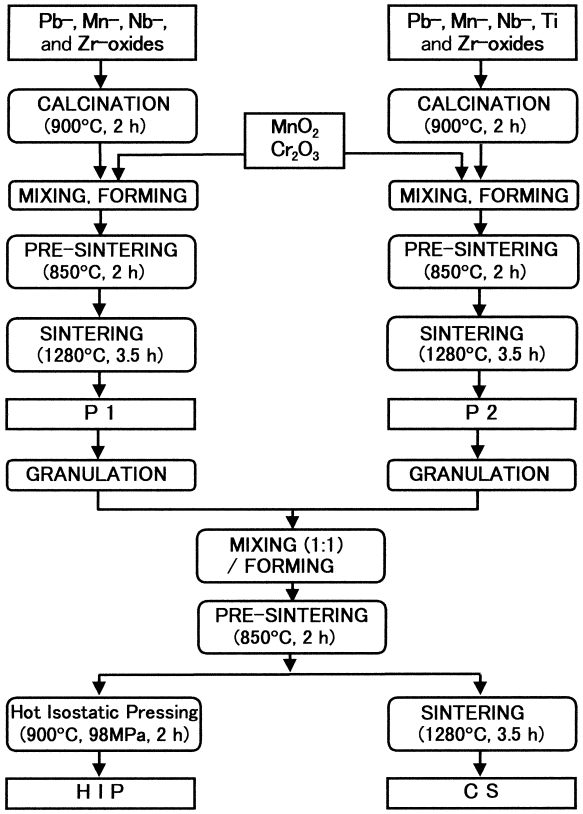

Fig. 1. Flow chart of sample preparation.

The samples were cut into tablets of 20 mm in diameter and 0·5 mm in thickness. Silver paste for electrode was painted on the both sides of the samples, and then the samples were polarized under 2×10^6 V/m bias at 80°C in a silicone oil bath for 1 h. Pyroelectric current (i) was measured in an electric oven at a heating rate of 2·0 C/min, and pyroelectric coefficient (P) was calculated from the following equation:[11]

$$P = \frac{\mathrm{d}Ps}{\mathrm{d}T} = \frac{i/A}{\mathrm{d}T/\mathrm{d}t} \tag{1}$$

where Ps is the spontaneous polarization, T the temperature, A the surface area of the electrode, and t the time.

The crystalline phases were identified through X-ray diffraction measurement (XRD) using Ni-filtered CuKα radiation together with the silicon powder as an internal standard. The fractured surfaces of the samples were etched in 18% HCl solution at 20°C for a period from 0 to 210 s, and then analyzed by X-ray photoelectron spectroscopy (XPS). A photoelectron spectrum from the Zr3d orbital was smoothed and deconvoluted using a Gaussian fitting program.

3 Results and Discussion

3.1 Pyroelectricity

The ferroelectricity of HIP sample has been confirmed thanks to electric displacement curves as a function of the applied field (D–E) which don't exhibit significant distortion.[10] The temperature dependence of the pyroelectric coefficient for the different samples is shown in Fig. 2. The starting materials, P1 and P2, exhibit pyroelectric peaks at 27°C and 48°C, respectively, corresponding to their phase transition temperatures. It was further shown that CS sample has a clear peak at 37°C between the transition temperatures of P1 and P2. Thus, it can be assumed that CS is a complete solid solution of P1 and P2. These three peaks were not observed in HIP sample (hybrid of P1 and P2) and then the pyroelectric coefficient, which was consistent with a simulated dotted line (Fig. 2), was insensitive to any change in temperature. The pyroelectric coefficient ranging from 7·5 to $11{\cdot}3\times10^{-4}\,\mathrm{C^{-1}m^{-2}{\cdot}C}$ between 15°C and 70°C is more than twice as much as the one of typical pyroelectric materials.[12,13] In general, the pyroelectric sensitivity is evaluated in terms of 'figure of merit,' $FM1$, which is given by

$$FM1 = \frac{P}{(\rho\cdot C\cdot\varepsilon_r)} \tag{2}$$

where P, ρ, C and ε_r are the pyroelectric coefficient, the density, the specific heat at constant volume and the relative permittivity, respectively. The $FM1$ of this sample was calculated to be about $2\times10^{-12}\,\mathrm{CmJ^{-1}}$, which is high enough compared with the values of 3·7 to $9{\cdot}0\times10^{-14}\,\mathrm{CmJ^{-1}}$ reported in the literature.[12,13]

3.2 Crystalline phase

In this study, the ionic radius of an A-site Pb^{2+} was 0·121 nm,[14] and the reduced ionic radii of B-site Zr^{4+}, Ti^{4+}, Nb^{5+} and Mn^{2+} were 0·0790 nm for P2 and 0·0793 nm for P1. From the phase diagram of $A^{2+}B^{4+}O_3$ perovskite crystal structure based on the ionic radii,[15] the crystal form of all the samples must belong to a pseudo-tetragonal system. This was confirmed from the complete

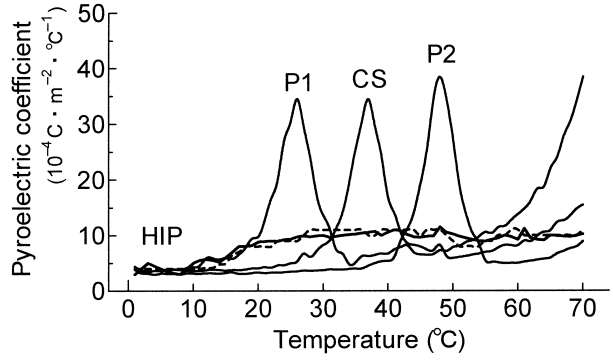

Fig. 2. Temperature dependence of the pyroelectric coefficients corresponding to P1, P2, CS, and HIP samples. A dotted line denotes a simulation curve by summation of the curves for P1, P2, and their six solid solutions of which the phase transition temperatures are 30, 33, 36, 39, 42, and 45°C.

Miller indices of the XRD profiles as a pseudo-tetragonal system, as shown in Fig. 3(a). Figure 3(b) shows further the detailed diffraction profiles around $2\theta = 67{\cdot}5°$ for the (221) and the (212) planes of the samples. The diffraction angles corresponding to these planes in the case of P1 were notably lower than those found for P2, as expected in taking into account the P1's large B-site ions, and the diffraction angles in the case of CS located solely between those of P1 and P2. Also, the profile of HIP was broadened, different from those of P1, P2, and CS. It could be considered as the sum of the contributions of the serial solid solutions between P1 and P2, because a lower diffusion temperature of 900°C here facilitated to suppress the formation of a complete solid solution. This consideration could be supported by a summation of the profiles for P1, P2, and CS, which was close to that for HIP. These solid solutions could result from a mutual substitution on the B-site ions. The serial solid solutions in HIP sample were expressed to be $Pb(Nb_{2/3}Mn_{1/3})_{0{\cdot}1}Zr_{0{\cdot}9-x}Ti_xO_3$ with $0 < x < 0{\cdot}025$.

3.3 Microstructure

Figure 4 shows a Zr3d binding energy spectrum obtained from the XPS profile of HIP sample. In general, the Zr3d spectrum consists of two peaks corresponding to two kinds of total angular momenta of electrons, 3/2 and 5/2, and then the difference between their binding energies and the ratio of their peak areas are approximately 2·5 eV and 2:3, respectively.[16] The deconvolution of the Zr3d spectrum of HIP sample based on the above description gave two sets of peak-pairs denoted as [A]; peak ① (181·3 eV) and peak ② (183·8 eV), and [B]; peak ③ (182·4 eV) and peak ④ (184·8 eV). A set of [A] appeared in all the samples, while a set of [B] did only in the P1-containing samples; P1, CN, and HIP. Here, CN sample was prepared by calcination (800°C, 1 h) of the mixture of P1 and P2 in order to obtain an XPS spectrum of the mixture for avoiding the formation of a solid solution between P1 and P2. That is, the appearance of the [B] must be an indicator of the contribution of the starting material, P1, without the Ti component to the XPS profile. The order of the area ratio [B] : [A] was P1 > CN > HIP > P2 = CS = zero. It was suggested that diverse changes of chemical bonding between a mixture and a complete solid solution occurred through the reaction of a part of P1 and P2 during HIP.

After being etched for 60 s, a pimple-like morphology was found only on the grain surface of HIP sample, and was attributed to a difference of the solubility between Ti and Zr components.[17] The difference of the solubility was further confirmed from inductively coupled plasma emission spectrometric (ICP) measurements of eluted ion concentrations in the etching solution. The pimple-like morphology also disappeared on the surface after being etched for 150 s. The thickness of the reacted layer was roughly estimated to be 100–500 nm from the mass of component ions eluted for

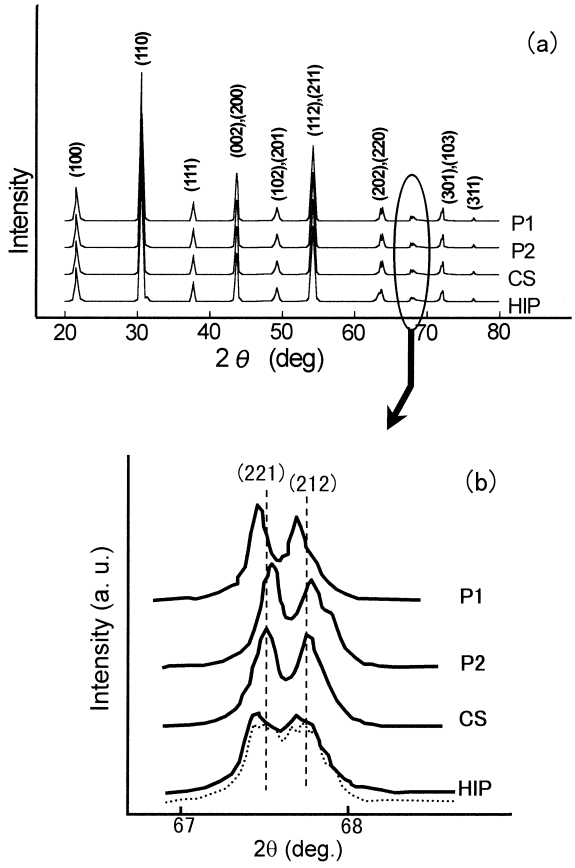

Fig. 3. X-ray diffraction profiles of P1, P2, CS and HIP samples. (a) From $2\theta = 20$–$80°$ (b) enlarged profiles at around $2\theta = 67{\cdot}5°$. (A dotted line denotes a simulation curve by summation of P1, P2, and CS curves.)

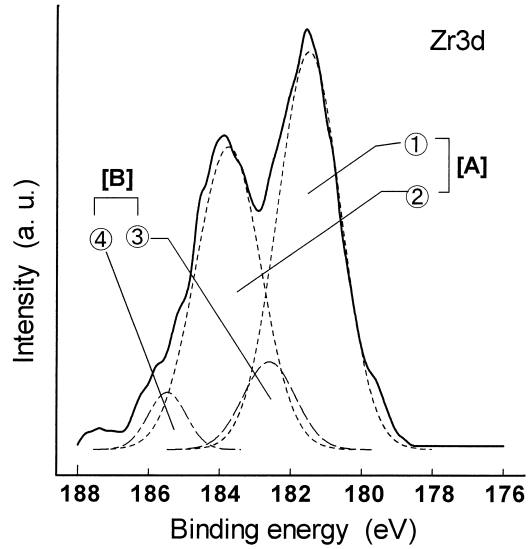

Fig. 4. XPS spectrum of Zr3d and its deconvolution of HIP sample. [A] is attributed to all the PZT-related ceramics in this study, and [B] is inherent in P1 together with [A], obtained by deconvolution.

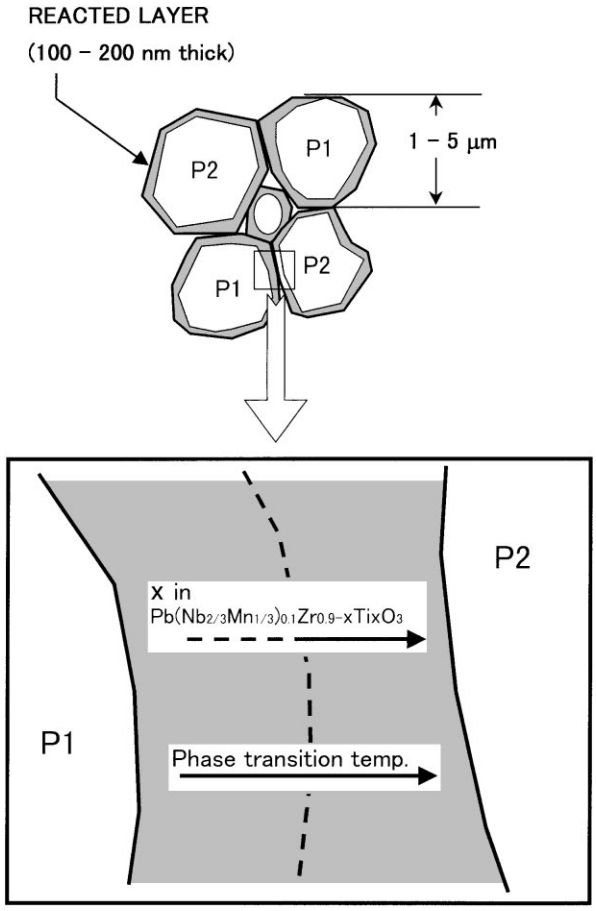

Fig. 5. Schematic drawing of reacted layer of HIP sample.

the etching time of 150 s in consideration of the elution behavior in this study. The percentage peak area of the [B] in Fig. 4 increased gradually with increasing etching time, and then saturated to the value of 21% at the time of 150 s. This percent was close to that of the mixture of P1 and P2, indicating that the reacted layer was thus eliminated almost completely by the etching for 150 s.

Figure 5 illustrates the schematic reaction model. The reaction layer of compositional gradient perpendicular to the grain boundary occurred on the grain surface. This compositional gradient results in the formation of a functional gradient material with the serial phase transition temperatures, that is, the diminishing of the temperature dependence of the pyroelectric coefficient was due to the overall integration of these numerous pyroelectric components in the compositional gradient layers. Further intensive enhancement of the pyroelectric sensitivity may be possible by means of the disordering of B-site ions in the perovskite ferroelectric materials, the same as the piezoelectricity reported by Yamashita *et al.*[18]

References

1. Porter, S. G., A brief guide to pyroelectric detectors. *Ferroelectrics*, 1981, **33**, 193–206.
2. Putley, E. H., The applications of pyroelectric devices. *Ferroelectrics*, 1981, **33**, 207–216.
3. Michel, C., Moreau, J. M., Achenbach, G. D., Gerson, R. and James, W. J., Atomic structure of two rhombohedral ferroelectric phases in the $Pb(Zr,Ti)O_3$ solid solution series. *Solid State Commun.*, 1969, **7**, 865–868.
4. Jaffe, B., Cook Jr, W. R. and Jaffe, H., Phase diagram of $Pb(Zr,Ti)O_3$ system. In *Piezoelectric Ceramics*. Academic Press, New York, 1971, p.136.
5. Adachi, M., Hachisuka, A., Okumura, N., Shiosaki, T. and Kawabata, A., Pyroelectric and dielectric properties of rhombohedral $Pb(Zr_{1-x}Ti_x)O_3$ ceramics. *Proc. of the 6th Meeting on Ferroelectrics Materials and Their Applications. Jpn. J. Appl. Phys.*, 1987, **26** (Suppl. 26-2), 68–71.
6. Ushida, Y., Lian, J., Shiosaki, T. and Kawabata, A., Ferro- and piezo-electric properties for $F_{R(LT)}$ to $F_{H(LT)}$ phase transition of PZT system. *Proc. of the 6th Meeting on Ferroelectrics Materials and Their Applications. Jpn. J. Appl. Phys.*, 1987, **26** (Suppl. 26-2), 72–75.
7. Komiya, H., Naito, Y., Takenaka, T. and Sakata, K., Piezoelectric and pyroelecric composite ceramics of the multilayer type by tape casting. *Proc. of the 7th Meeting on Ferroelectrics Materials and Their Applications. Jpn. J. Appl. Phys.*, 1989, **28** (Suppl. 28-2), 114–116.
8. Takenaka, T., Komiya, H. and Sakata, K., $PbZrO_3$-based composite pyroelectric ceramics. *Proc. of the 7th IEEE International Symposium on Applied Ferroelectrics*, 1991, pp. 370–373.
9. Lian, J., Okumura, N., Adachi, M., Shiosaki, T. and Kawabata, A., Mixed sintering of $PbZrO_3$ rich PZT ceramics and their pyroelectric properties. *Proc. of the 7th IEEE International Symposium on Applied Ferroelectrics,* 1991, pp. 383–386
10. Sugiyama, O., Ohtake, M., Kuwahara, H., Ohsumi, S., Kato, K., Fukushima, T. and Kaneko, S., Modification and pyroelectricity of $Pb(Zr,Ti)O_3$-based ceramics using HIP with novel glass encapsulation. *J. Ceram. Soc. Jpn.* 1996, **104**, 486–489.
11. Byer, R. L. and Roundy, C. B., Pyroelectric coefficient direct measurement technique and application to a nsec response time detector. *Ferroelectrics,* 1972, **3**, 333–338.
12. Hardiman, B., Kiehl, K. V., Reeves, C. P. and Zeyfang, R. R., Lead titanate zirconate-based pyroelectric ceramics. *Ceramurgia Int.*, 1978, **4**, 108–112.
13. Beerman, H. P., Investigation of pyroelectric material characteristics for improved infrared detector performance. *Infrared Physics*, 1975, **15**, 225–231.
14. Pauling, L., Table of ionic radii. In *The Nature of The Chemical Bond,* 3rd ed. Cornell University Press, Ithaca, 1960, p. 514.
15. Roth, R. S., Classification of perovskite and other ABO_3-type compounds. *J. Res. NBS,* 1957, RP2736, **58**, 75–88.
16. Moulder, J. F., Stickle, W. F., Sobol, P. E. and Bomben, K. D., Figure of typical Zr_{3d} spectrum. In *Handbook of X-ray Photoelectron Spectroscopy*, ed. J. Chastain. Perkin–Elmer, Minnesota, USA, 1992, p. 109.
17. Sugiyama, O., Saito, S., Kato, K., Ohsumi, S., Murakami, K. and Kaneko, S., Microstructure of $Pb(Zr,Ti)O_3$-based ceramics HIPped with glass encapsulation. *Jpn. J. Appl. Phys.*, 1997, **36**, (Part 1, No.9B), 5984–5988.
18. Yamashita, Y., Harada, K., Hosono, Y., Natsume, S. and Ichinose, N., Effects of B-set ions on the electromechanical coupling factors of $Pb(B'B'')O_3$–$PbTiO_3$ piezoelectric materials. *Jpn. J. Appl. Phys.*, 1998, **37** (Part 1, No 9B), 5288–5291.